# The miR-145–MMP1 axis is a critical regulator for imiquimod-induced cancer stemness and chemoresistance

Shan Zhu [a],[1], Ning Yang [a],[1], Chao Niu [b], Wan Wang [a], Xue Wang [a], Junge Bai [c], Yuan Qiao [a], Shuanglin Deng [d], Yi Guan [d], Jingtao Chen [a],[*]

[a] *Institute of Translational Medicine, The First Hospital of Jilin University, Changchun 130061, China*
[b] *Department of Cancer Center, The First Hospital of Jilin University, Changchun 130024, China*
[c] *Department of Colorectal Surgery, The Forth Affiliated Hospital of Harbin Medical University, Harbin 150040, China*
[d] *Department of Neurosurgery, The First Hospital of Jilin University, Changchun 130024, China*

## A R T I C L E   I N F O

## A B S T R A C T

Cancer stemness, chemoresistance, and metastasis are related biological events. However, whether they have common molecular mechanisms remains to be determined. Here, we report that imiquimod (IMQ) facilitates the acquisition of stem-cell-like properties and chemoresistance via the upregulation of matrix metalloproteinase 1 (MMP1) and downregulation of microRNA-145 (miR-145). MiR-145–5p was found to suppress MMP1 expression through direct binding, and miR-145-mediated downregulation of MMP1 reversed the effects of IMQ. In addition, IMQ downregulated miR-145 by promoting DNA methylation at its promoter. DNA methyltransferase inhibitors limited IMQ-induced MMP1 expression, stemness, and chemoresistance. Collectively, our results highlight the miR-145–MMP1 axis as a potential coordinator of cancer stemness and chemoresistance. Given the role of MMP1 in the initiation of metastasis, the miR-145–MMP1 axis serves as a promising therapeutic target for improved cancer treatment.

## 1. Introduction

Cancer stemness properties, treatment resistance, and metastasis are involved in cancer progression and recurrence [1–3]; these biological events are interconnected and influence one another. It is well accepted that cancer stem cells (CSCs) are often resistant to conventional chemotherapy [4]; in recent years, several studies have also found associations between treatment resistance and metastasis [5,6], as well as between stemness and metastasis [7,8]. It has further been suggested that the molecules and signaling pathways might be common to these three events, providing promising therapeutic targets for improved cancer treatment.

Matrix metalloproteinase 1 (MMP1), a member of the matrix metalloprotease (MMP) family, is overexpressed in various cancer types [9, 10]. High MMP1 expression is a conventional marker of the epithelial-mesenchymal transition (EMT) and is associated with tumor metastasis [11,12]; in this process, microRNAs (miRNAs) are involved in the transcriptional regulation of MMP1, either directly or indirectly [10, 13,14]. MMP1 is essential for the migratory activities of mesenchymal stem cells (MSCs), and its functional inactivation abrogates MSC tumor tropism [15,16]. In cancer cells and CSCs, MMP1 levels are positively correlated with the expression levels of stem cell markers [17,18]. However, the functional role of MMP1 in cancer cell stemness has not been definitively established. Similarly, although EMT is known to be associated with chemoresistance [19,20], the involvement of MMP1 in chemoresistance is less well understood.

As a tumor suppressor miRNA, miR-145 is expressed at low levels in various human malignancies, including breast cancer [21], colorectal cancer [22], lung cancer [23], glioblastoma [24], and prostate cancer [25]. A low level of miR-145 contributes to tumor metastasis [21,26,27] and is associated with a high risk of recurrence and poorer survival [24, 28,29]. Notably, miR-145 negatively modulates cancer cell stemness by

regulating its target genes, which include some stemness-related markers (e.g., *CD44* [30] and *SOX2* [31]), as well as pluripotency-related genes (e.g., *Oct4* [32]). The expression of miR-145 is affected by post-transcriptional control as well as transcriptional regulation. In cancer cells, DNA hypermethylation has been reported to be closely related to miR-145 downregulation [21,33].

Imiquimod (IMQ) is a small-molecule immunomodulator with anti-tumor effects. IMQ cream has been used to treat superficial skin cancers [34]. Previous studies have suggested that IMQ could directly induce cancer cell apoptosis or proliferation in distinct tumor types [35]. We previously reported that IMQ could increase the stemness of glioma stem cell (GSC)-like cells via GDF15-mediated activation of the LIF–STAT3 pathway [36]. However, the regulatory effect of IMQ on stemness in differentiated cancer cells remains to be explored.

In this study, we demonstrated that IMQ promotes the acquisition of CSC-like properties in differentiated cancer cells while reducing the sensitivity of cancer cells to chemotherapy. Through data mining, we found that IMQ upregulates MMP1 expression by inhibiting miR-145 transcription. Then, we investigated the specific molecular mechanism by which miR-145–5p targets MMP1 and the miR-145–MMP1 axis to modulate stemness and chemoresistance in IMQ-treated cancer cells. These findings provide evidence that a regulatory network involving the miR-145–MMP1 axis might be common to cancer stemness, chemoresistance, and metastasis.

## 2. Materials and methods

### 2.1. Cell lines and cell culture

Cell lines U87, T98G, and HCT116 were purchased from Procell Life Science & Technology Co., Ltd. (Wuhan, China). All cell lines were authenticated using short tandem repeat profiling. Cells were cultured in Dulbecco's modified Eagle's medium (DMEM; HyClone, Logan, UT, USA) supplemented with 10% fetal bovine serum (FBS; Biological Industries, Kibbutz Beit Haemek, Israel), 100 U/mL penicillin (HyClone), and 100 μg/mL streptomycin sulfate (HyClone). U87-Luc cells transduced with a luciferase gene were cultured in DMEM supplemented with 10% FBS, and the culture medium was further supplemented with 1 μg/mL puromycin (Life Technologies, Grand Island, NY, USA).

### 2.2. RNA isolation and quantitative PCR (qPCR)

Total RNA was extracted using an EasyPure RNA Kit (Transgen Biotech Co., Ltd., Beijing, China), cDNA was synthesized using the TransScript First-Strand cDNA Synthesis SuperMix (Transgen Biotech Co., Ltd.), and miRNAs were reverse-transcribed using TransScript miRNA First-Strand cDNA Synthesis SuperMix (Transgen Biotech Co., Ltd.). qPCR was performed using FastStart DNA Master SYBR Green (Roche Diagnostics, Indianapolis, IN, USA) on an ABI Plus Real-Time PCR System (Applied Biosystems, Foster City, CA, USA). The primers used (Supplementary Table 1) were synthesized by Comate Bioscience (Changchun, China). Samples were analyzed in triplicate.

### 2.3. Western blotting

Samples were washed with ice-cold phosphate-buffered saline and lysed in radioimmunoprecipitation lysis buffer (Cell Signaling Technology, Danvers, MA, USA) on ice for 30 min. The samples were prepared for loading by adding 5 × sample buffer (Invitrogen, Carlsbad, CA, USA) and heating at 100°C for 10 min. Equal amounts of cell lysates were resolved using sodium dodecyl sulfate-polyacrylamide gel electrophoresis and transferred onto polyvinylidene difluoride membranes. After blocking with 5% bovine serum albumin, the blots were incubated with primary antibodies overnight at 4°C. The following day, secondary antibodies diluted in blocking buffer were added and incubated for 1 h at room temperature. Specific protein bands were visualized using Western Lightning Plus-ECL (Perkin Elmer Biosciences, Waltham, MA, USA) on a ChemiDoc™ Imaging System (Bio-Rad, Hercules, CA, USA).

Anti-CD133 (Invitrogen, #PA5–38014), anti-SOX2 (R&D System, Minneapolis, MN, USA, #MAB2018), anti-MMP1 (Proteintech, Wuhan, China, #10371–2-AP), and anti-β-actin (Transgen, #HC201–02) were the primary antibodies used. Horseradish peroxidase-labeled anti-mouse IgG (#AB150113) or anti-rabbit IgG antibodies (#AB150080) (Perkin Elmer Biosciences, Boston, MA, USA) were used as secondary antibodies.

### 2.4. Infection and transfection

Adenoviruses harboring pre-miR-145 (adv-miR-145) and a non-specific control were obtained from Vigene Biosciences (Shandong, China). After infection with 40 MOI of adv-miR-145 or control for 72 h, the cells were harvested for subsequent experiments.

For short interfering RNA (siRNA) transfection, cells were plated (2 × 10⁵/well) in six-well plates. The following day, cells were transfected with 160 nmol MMP1 siRNA or scrambled control using 6 μL of jet-PRIME transfection reagent (Polyplus-transfection SA, Illkirch, France) in 200 μL of jetPRIME buffer. After 72 h, the knockdown efficiency was verified.

### 2.5. Luciferase reporter assay

Synthetic oligonucleotides were generated for the 3′- and 5′-untranslated regions (UTRs) of wild-type *MMP1* with potential miR-145–5p binding sites or mutants of each binding site (Supplementary Table 2) and cloned into the pMIR-REPORT luciferase vector. HEK293T cells were seeded into 96-well plates and infected with miR-145–5p. After 6 h, the medium was replaced with normal medium and cultured overnight. The next day, the pMIR-REPORT luciferase vector and Renilla plasmid were co-transfected into the HEK293T cells using jetPRIME transfection reagent for 6 h, followed by culture in normal media for 48 h. For the luciferase reporter assay, the cells were harvested and lysed, and the luciferase activity was assessed using a Dual-Luciferase Reporter Assay System (Transgene) and normalized to Renilla luciferase activity as per the manufacturer's protocol.

### 2.6. Bisulfite sequencing PCR (BSP)

Genomic DNA was extracted from cells using a TIANamp Genomic DNA kit (Tiangen Biotech, Beijing, China) and then treated with bisulfite according to the EZ DNA Methylation-Gold™ Kit instruction manual (ZYMO Research, Freiburg, Germany). Specific regions of the BSP promoter construct containing the miR-145 promoter fragment were amplified using PCR; the sequences of the primers used for PCR are shown in Supplementary Table 3. After purification, the PCR products were cloned into pEASY-T1 and sequenced.

### 2.7. Immunofluorescence

Cells were cultured in 35 mm glass-bottom cell culture dishes (NEST, Wuxi, China) and incubated in medium containing IMQ for 5 days. The cells were then stained using standard procedures. Samples were first incubated with primary antibodies at 4°C overnight and subsequently with the corresponding Alexa Fluor-conjugated secondary antibody (1:1000 dilution) for 1 h at room temperature. Nuclei were counterstained with 4′,6-diamidino-2-phenylindole (DAPI, Life Technologies), and the dishes were observed under a confocal microscope (Olympus FV3000; Olympus, Tokyo, Japan).

### 2.8. In vivo tumor studies

NOD/SCID mice (female; 12–14 weeks old) were purchased from Vital River Laboratory Animal Technology Co. (Beijing, China). Animal

experiments were performed according to institutional guidelines and were approved by the ethics committee of The First Hospital of Jilin University (license No.: 2018-042). To investigate the effects of IMQ treatment on the survival of tumor-bearing mice, NOD/SCID mice were subcutaneously injected with U87-Luc cells ($2 \times 10^6$/mouse) in 0.1 mL of saline on their right flank. The occurrence of glioma was confirmed via bioluminescence imaging on day 5 after inoculation, after which the tumor-bearing mice were randomly divided into two groups. Mice were intratumorally injected with IMQ VacciGrade (20 µg each; InvivoGen, San Diego, CA, USA) in 30 µL saline (IMQ group) or with 30 µL saline (saline group) on days 10, 12, 14, 16, 18, 20, and 22 after tumor cell inoculation. Subsequently, tumor growth was measured with calipers every 2 days, and the tumor volumes were calculated using the following formula: $V = [(\text{length}) \times (\text{width})^2]/2$.

### 2.9. Sphere formation assay

Cells (500 cells/well) were seeded into six-well ultra-low-attachment plates (Corning, Inc., Corning, NY, USA) and cultured in a chemically defined serum-free medium containing DMEM/F12 base (Thermo Fisher Scientific, San Jose, USA), $1 \times$ N2 (Thermo Fisher Scientific), $1 \times$ B27 (Thermo Fisher Scientific), 20 ng/mL EGF (PeproTech, Rocky Hill, USA), 20 ng/mL bFGF (PeproTech), and 2.5 mg/mL heparin (Life Technologies). After 14 days of culture, primary tumorspheres with diameters > 70 µm were counted. During passaging, tumorspheres were harvested via centrifugation, digested with Accutase solution (Sigma-Aldrich, St. Louis, MO, USA), and then reseeded (500 cells/well) to develop secondary spheres after another 14 days of growth. This procedure was repeated for ternary tumorspheres.

### 2.10. Chemosensitivity assay

The 3-(4,5-dimethyl-2-thiazolyl)-2,5-diphenyl-2 H-tetrazolium bromide (MTT) assays were performed to evaluate the chemosensitivity of cancer cells. Briefly, cells were plated in 96-well plates at a density of $3.5 \times 10^3$ cells/well overnight. The following day, chemotherapeutic agents were added to the culture medium, and the cells were incubated for 4 days. Cell growth was evaluated using MTT staining (Sigma-Aldrich). Following 4 h incubation, the medium was removed and dimethyl sulfoxide was added. The optical density at 490 nm was measured using a microplate reader (Biotech Instruments, Winooski, VT, USA), and half-maximal inhibitory concentrations ($IC_{50}$) values were calculated using GraphPad Prism v7 (GraphPad Software Inc., La Jolla, CA, USA).

### 2.11. Statistical analysis

Data are presented as the mean ± SEM and were analyzed using Student's *t*-test or one-way analysis of variance (ANOVA) followed by Tukey's post-hoc test. Statistical analyses were performed using GraphPad Prism v7.

## 3. Results

### 3.1. IMQ upregulates MMP1 via miR-145 downregulation in cancer cells

To assess the functional effect of the immunomodulator IMQ on cancer cell stemness, we obtained U87-derived tumorsphere cells (named U87 TS) under hypoxic (5% $O_2$) conditions in serum-free culture; U87 TS cells have been characterized as GSC-like cells with phenotypic and functional features of GSC [36]. RNA-sequencing (RNA-seq) was then performed to analyze gene expression changes in U87 TS cells after 5 days of IMQ treatment. The RNA-seq data revealed that the MMP1 level was upregulated more than four-fold following IMQ treatment (Fig. 1A). Consistent with the RNAseq data, IMQ enhanced the mRNA and protein levels of MMP1 in U87 TS, U87 (glioma cells), T98G

(glioma cells), and HCT116 (colon cancer) cells (Fig. 1B–C). Moreover, RNAseq analysis demonstrated that IMQ suppressed the expression of miR143HG (the host gene for both miR-143 and miR-145) in IMQ-treated U87 TS cells (Fig. 1A). We further confirmed that IMQ significantly downregulated the expression of miR-145–5p (the guide strand) by approximately 60% in U87 TS and normal cancer cells (Fig. 1D–E). MMP1 has been predicted to be a target of miR-145 [37,38]. Indeed, we verified that the adenovirus-mediated overexpression of pre-miR-145 (adv-miR-145) significantly inhibited MMP1 expression in cancer cells (Fig. 1F–G). In addition, MMP1 upregulation in IMQ-treated cells was markedly repressed upon overexpression of miR-145 (Fig. 1H–I). Taken together, these data indicate that high levels of MMP1 in cancer cells might depend on miR-145 suppression.

### 3.2. MiR-145 targets MMP1 by directly binding to both the 3′- and 5′-UTRs of the MMP1 transcript

Previous findings showed that the increase in miR-145 levels was paralleled by an MMP1 decrease [37,38]; however, this did not verify a direct interaction between miR-145–5p and *MMP1* mRNA. Using the BiBiserv server software (https://bibiserv.cebitec.uni-bielefeld.de/index.html), we predicted that both the 3′-UTR and 5′-UTR of *MMP1* mRNA would have binding sites for miR-145–5p (Fig. 2A). Subsequently, both UTRs of *MMP1* (containing wild-type or mutant binding sites for miR-145–5p) were cloned into separate luciferase reporter plasmids separately (Fig. 2B). In dual-luciferase reporter assays, plasmids containing either UTR alone (either 3′ or 5′) bound to miR-145–5p, thereby reducing the relative luciferase reporter activity; by contrast, plasmids bearing mutated binding sites (either 5Um or 3Um) failed to repress the relative luciferase reporter activity, suggesting that both *MMP1* UTRs have binding sites for miR-145–5p (Fig. 2C). Remarkably, the plasmids containing both *MMP1* UTRs (5ULuc3U) showed a significant change in luciferase reporter activity compared with plasmids containing Luc3U or 5ULuc alone (Fig. 2D). These data demonstrate that miR-145 binds to 3′-UTR and 5′-UTR of *MMP1* mRNA and that the two binding modes act synergistically on MMP1 transcriptional repression.

### 3.3. MiR-145-mediated MMP1 downregulation reverses the acquisition of stem cell-like properties of IMQ-treated cells

Our previous work confirmed that IMQ promoted the stemness of GSC-like cells [36]. In differentiated cancer cells, IMQ downregulates the level of miR-145; the latter participates in the regulation of cancer stemness [30–32]. Therefore, we postulated that IMQ stimulation could result in the acquisition of stemness in differentiated cancer cells. Indeed, we observed that IMQ treatment significantly upregulated the expression of stemness markers (Fig. 3A–B). Immunofluorescence results showed a more pronounced expression of CD133 in the membrane and cytoplasm of cancer cells following IMQ treatment. Meanwhile, upregulated SOX2 was primarily observed within the nucleus (Fig. 3C). Furthermore, IMQ promoted tumorsphere formation (Fig. 3D). Next, we used a subcutaneous xenograft mouse model to assess the *in vivo* effect of IMQ treatment on glioma cells. The survival of mice receiving IMQ injection was significantly shorter than that of control mice (Fig. 3E). Both CD133 and SOX2 levels increased in the IMQ-treated group tumor compared with those in the control group tumor tissues (Fig. 3F). These results indicate that IMQ enhances the stemness of glioma cells both *in vivo* and *ex vivo*.

To assess the functional role of MMP1 in IMQ-induced stemness, we silenced endogenous *MMP1* in cancer cells using two commercially available siRNAs that target different regions of the gene. As shown in Fig. 4A, high levels of cancer stem markers in IMQ-treated cells were significantly suppressed by MMP1 silencing; similar results were observed with miR-145 overexpression (Fig. 4B). Moreover, as expected, MMP1 silencing effectively inhibited tumorsphere formation in IMQ-treated cells (Fig. 4C). These observations suggest that the miR-
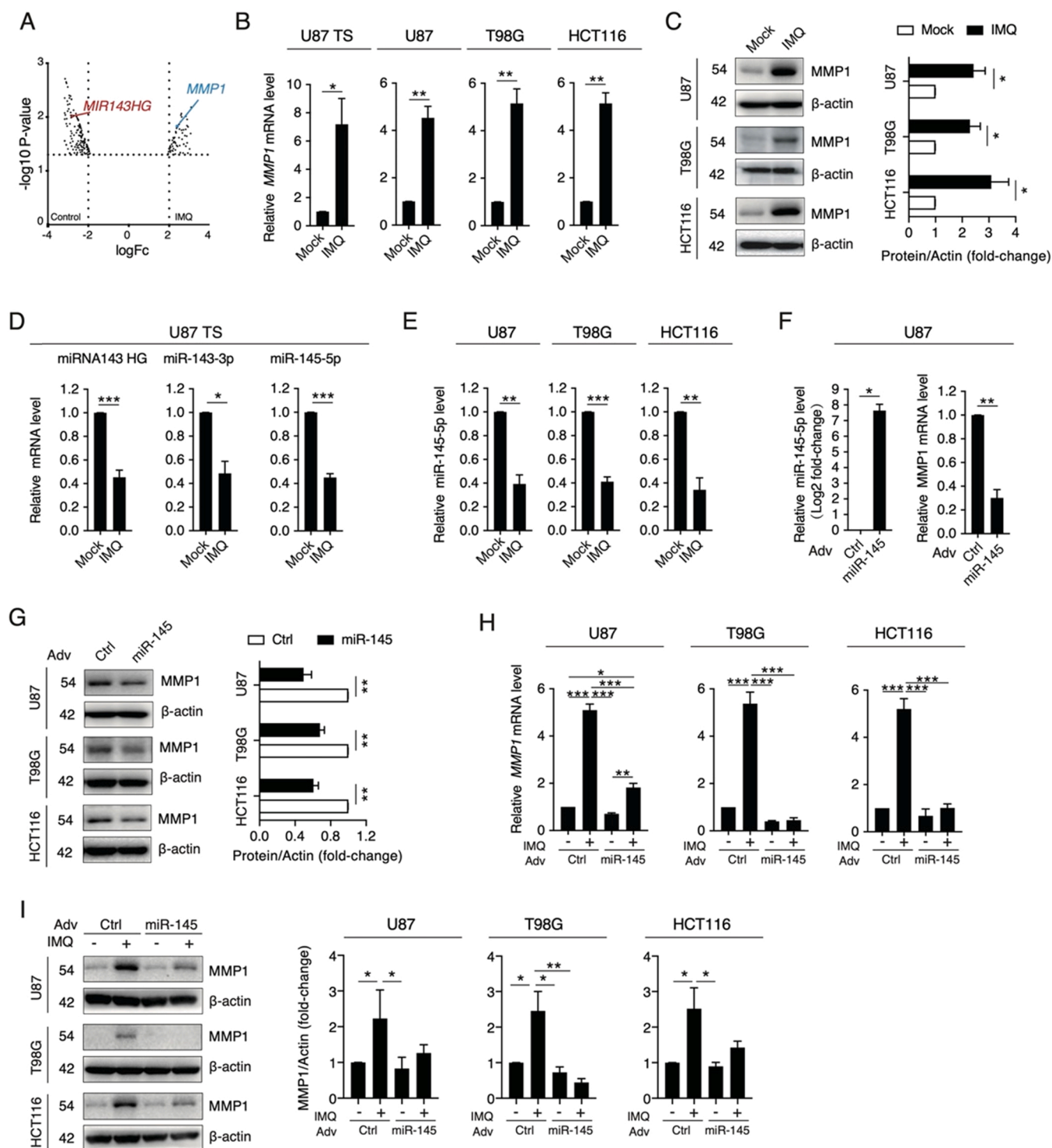
**Fig. 1.** Imiquimod (IMQ) upregulates matrix metalloproteinase 1 (MMP1) and downregulates miR-145, whereas overexpression of miR-145 suppresses MMP1 expression in cancer cells. (A) Volcano plot of differentially expressed genes in control and U87 TS cells treated with 5 μg/mL imiquimod (IMQ). (B) qPCR analysis of MMP1 expression in U87 TS, U87, T98G, and HCT116 cells treated with 5 μg/mL IMQ. (C) Western blot analysis and statistical evaluation of MMP1 levels in cancer cells after treatment with IMQ. (D) qPCR analysis of miR-143 HG, miR-143–3p, and miR-145–5p levels in control and IMQ-treated U87 TS cells. (E) qPCR analysis of miR-145–5p levels in control and IMQ-treated U87, T98G, and HCT116 cells. (F) qPCR analysis of miR-145–5p levels and MMP1 expression in U87 cells with adenoviruses harboring pre-miR-145 (adv-miR-145). (G) Western blot analysis and statistical evaluation of MMP1 levels in cancer cells overexpressing miR-145. (H–I) qPCR and western blot analysis of MMP1 level in cancer cells treated with IMQ after adenovirus-mediated overexpression of pre-miR-145. Values in (B–I) are from three independent experiments and are presented as the mean ± SEM; * $p < 0.05$, ** $p < 0.005$, *** $p < 0.0005$. Unpaired *t*-test (B–G); one-way ANOVA with Tukey's multiple comparison test (H–I).
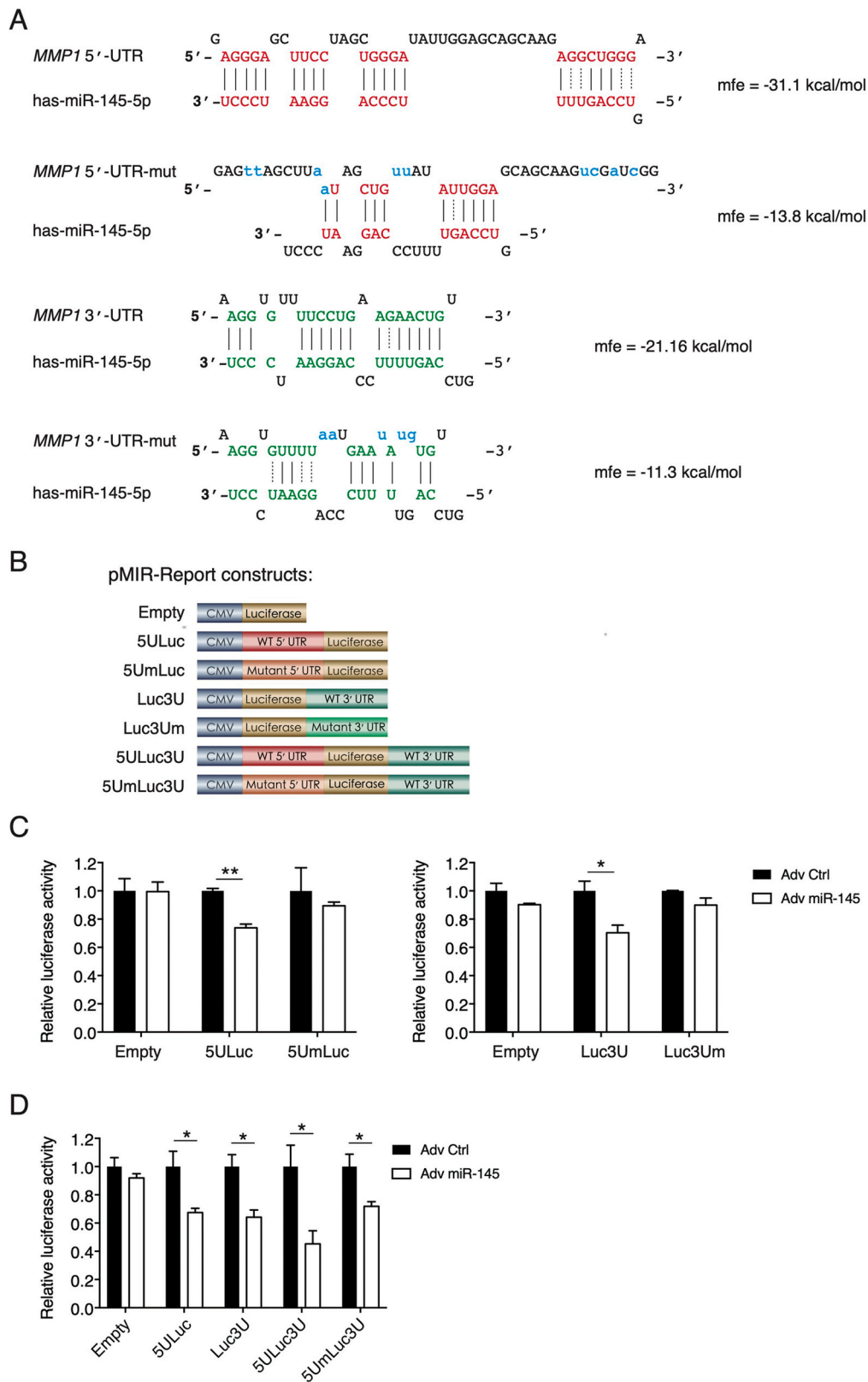
**Fig. 2.** Matrix metalloproteinase 1 (*MMP1*) is a direct target of miR-145–5p, which binds to both untranslated regions (UTRs) of *MMP1* mRNA. (A) MMP1 was determined to be the primary target of miR-145–5p. MMP1 possesses binding sites for miR-145–5p in its 3′- and 5′- UTRs. (B) Schematic depiction of luciferase reporter vectors containing wild-type and mutant 3′- and 5′-UTRs of *MMP1*. (C–D) Luciferase activity was detected in HEK293T cells co-transfected with the indicated reporter plasmids and pre-miR-145. *Renilla* luciferase activity was normalized to firefly luciferase activity as a control for transfection efficiency. Values in (C–D) are presented as the mean ± SEM. * $p < 0.05$, ** $p < 0.005$; unpaired *t*-test.
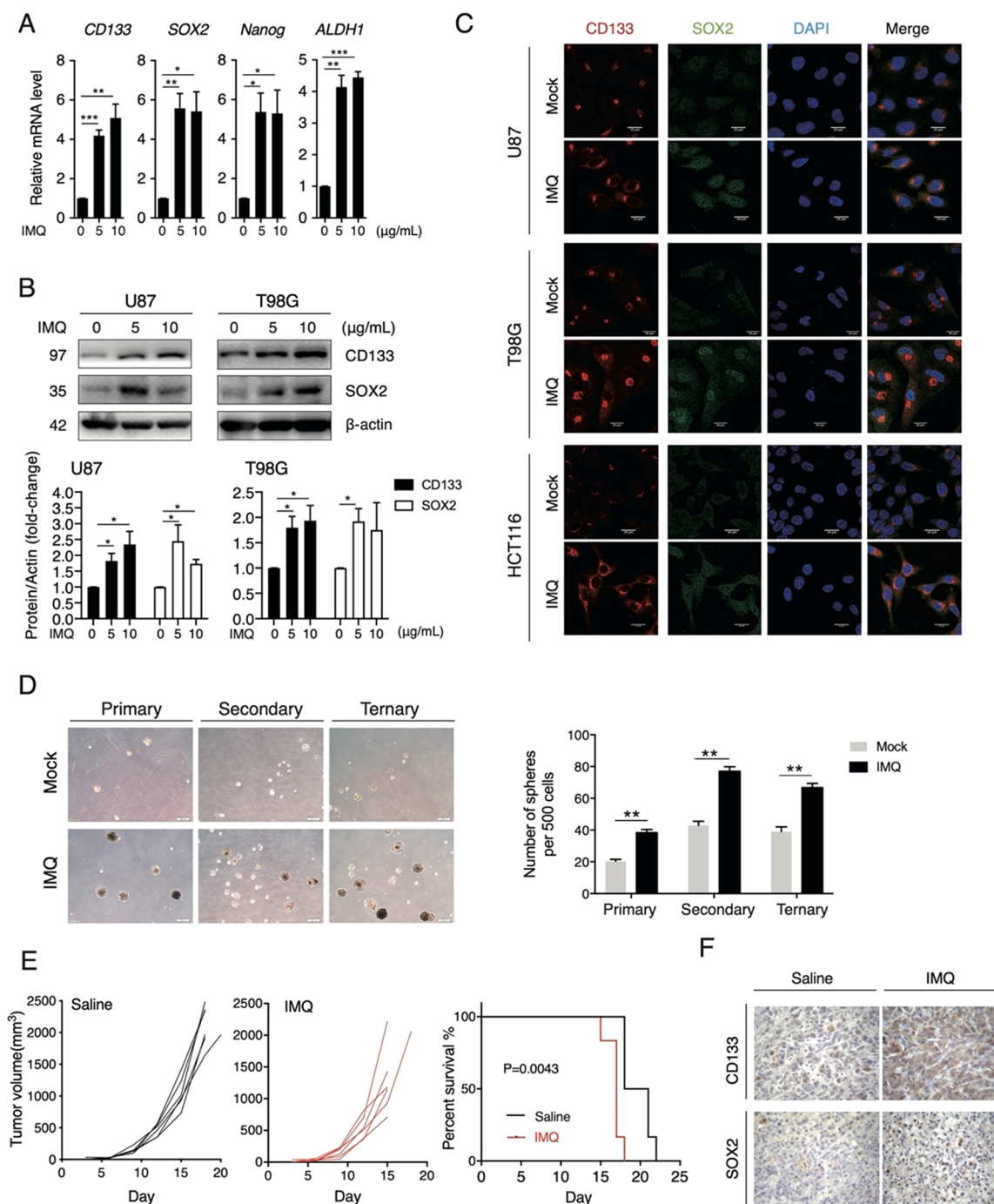
**Fig. 3.** Imiquimod (IMQ) facilitates the acquisition of stem cell-like properties of cancer cells. (A) qPCR analysis of *CD133*, *SOX2*, *Nanog*, and *ALDH1* expression in U87 cells treated with 0, 5, or 10 μg/mL IMQ. (B) Western blot analysis and statistical evaluation of CD133 and SOX2 levels in U87 and T98G cells after treatment with IMQ. (C) Representative images of U87, T98G, and HCT116 cells treated with 5 μg/mL IMQ for 5 days. Immunofluorescence was performed with anti-CD133 (red) and anti-SOX2 (green) antibodies with 4′,6-diamidino-2-phenylindole (DAPI) staining (blue). Scale bar = 20 μm. (D) Sphere formation assays were used to analyze the sphere-forming rates of the control and IMQ-treated U87 cells. Left: representative images of the rates of sphere formation. Right: the sphere-forming rate was assessed at the indicated times by sphere counting. (E) Tumor growth curve and survival curve in the saline and IMQ groups. Tumor volumes were determined using external calipers, and growth curves for U87 xenografts in NOD/SCID mice were plotted (n = 6 mice per group). Data were analyzed using the log-rank test (survival curve comparison). (F) Immunohistochemical staining for CD133 and SOX2 in mice bearing subcutaneous U87 tumors. Values in (A–B and D) are from three independent experiments and are presented as the mean ± SEM; * $p < 0.05$, ** $p < 0.005$, *** $p < 0.0005$; unpaired *t*-test.

145–MMP1 axis is involved in the regulation of cancer stemness in differentiated cancer cells.

### 3.4. The miR-145–MMP1 axis mediates the chemoresistance of IMQ-treated cells

Cancer cells with high stemness properties often exhibit resistance to conventional chemotherapy. To elucidate whether IMQ confers chemoresistance in cancer cells, we generated dose-response curves for two
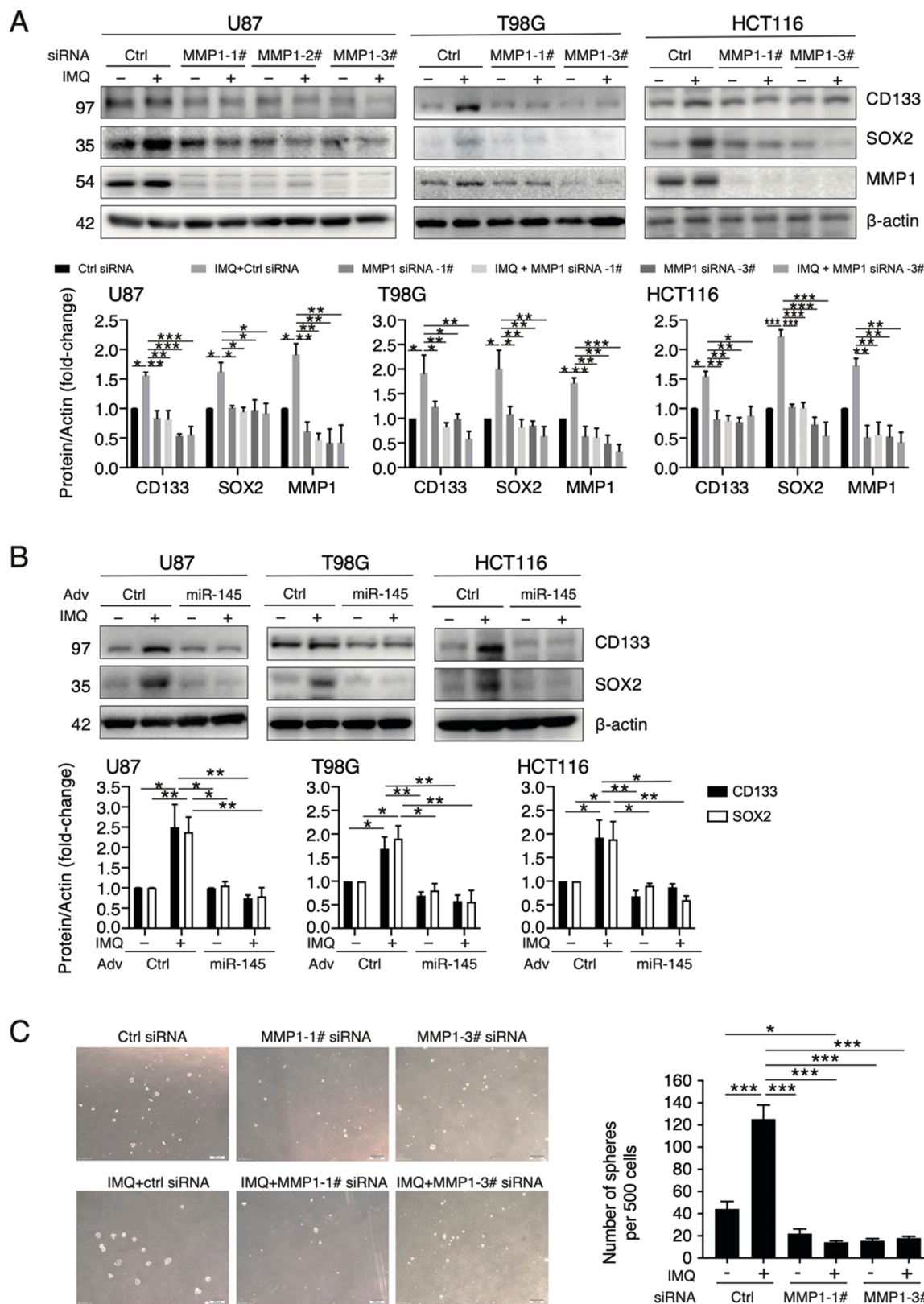
**Fig. 4.** Matrix metalloproteinase 1 (MMP1) silencing blocks the stemness-promoting effects of imiquimod (IMQ) in cancer cells. (A) Western blot analysis and statistical evaluation of CD133, SOX2, and MMP1 levels in cancer cells after treatment with IMQ and MMP1 siRNA or control siRNA. (B) Western blot analysis and statistical evaluation of CD133 and SOX2 protein levels in cancer cells after treatment with IMQ and control adenovirus or miR-145-expressing adenovirus. (C) Sphere formation assays were performed in siRNA-transfected U87 cells in the presence or absence of IMQ. Values in (A–C) are from three independent experiments and presented as the mean ± SEM; * $p < 0.05$, ** $p < 0.005$, *** $p < 0.0005$; one-way ANOVA with Tukey's multiple comparison test.

broad-spectrum chemotherapeutic agents and calculated their $IC_{50}$ values. As shown in Fig. 5A–B, IMQ reduced the sensitivity of cancer cells to the chemotherapeutic agent cisplatin and doxorubicin (DOX). According to the results of the Annexin V apoptosis assay, IMQ protected U87 cells from cisplatin-induced apoptosis (Fig. 5C). Next, we aimed to determine whether the miR-145–MMP1 axis mediated the chemoresistance of IMQ-treated cells. MMP1 was silenced using siRNA in IMQ-treated cells; then, the cells were treated with chemotherapeutic agents. The results showed that IMQ-treated cells were not sensitive to cisplatin or DOX; however, this situation was effectively reversed by MMP1 silencing (Fig. 5D). Similarly, miR-145 overexpression limited the chemoresistance of IMQ-treated cells (Fig. 5E). Overall, these results demonstrate that the miR-145–MMP1 axis could be a critical factor in chemoresistance of cancer cells.

### 3.5. IMQ-induced miR-145 promoter hypermethylation contributes to MMP1 expression, cancer stemness, and chemoresistance

To further investigate the mechanism of miR-145 regulation by IMQ, we probed several essential steps of miR-145 transcription and found that IMQ upregulated DNA methylation of the miR-145 promoter region in glioma cells and colon cancer cells (Fig. 6A). Next, we used two DNA methyltransferase (DNMT) inhibitors, 5-azacytidine (5-Aza) and decitabine (DAC) to determine whether miR-145 suppression depended on promoter DNA methylation. As shown in Fig. 6B, both DNMT inhibitors significantly upregulated miR-145 levels and reversed the IMQ-induced miR-145 suppression. Moreover, the MMP1 upregulation in IMQ-treated cells was significantly attenuated by DNMT inhibitors (Fig. 6C–D). Overall, these results suggest that IMQ suppresses miR-145 expression by enhancing its promoter methylation, which also increases expression of MMP1, and DNMT inhibitors could also indirectly regulate MMP1 expression.

Finally, we tested whether miR-145 promoter hypermethylation was sufficient for cancer stemness and chemoresistance. As expected, DNMT inhibitors impeded the upregulation of stem marker levels and restored the sensitivity to chemotherapeutic agents in IMQ-treated cells (Fig. 7A–B). These results suggest that DNMT inhibitors can attenuate or overcome cancer stemness and chemoresistance by reversing the effects of the miR-145–MMP1 axis.

## 4. Discussion

The role of MMP1 in cancer invasion and metastasis has been established [10,39]; however, the exact functions of MMP1 in the regulation of cancer stemness and chemoresistance remain nebulous. In this study, we found that miR-145-mediated MMP1 downregulation reversed the acquisition of stem cell-like properties and chemoresistance in IMQ-treated cells, enabling us to elucidate the molecular mechanisms underlying the miR-145–MMP1 axis in the regulation of cancer cell stemness and chemoresistance. Several studies have also found associations between chemoresistance and metastasis [5,6], as well as between stemness and metastasis [7,8]. In light of this and the role of MMP1 in initiating metastasis [10,39], it could be speculated that the miR-145–MMP1 axis is common to cancer stemness, chemoresistance, and metastasis. Thus, the miR-145–MMP1 axis is a promising therapeutic target that could be used to improve cancer treatment.

MicroRNAs act directly or indirectly on MMP1 regulation [10,13, 14]. An earlier study confirmed that elevated miR-145 expression reduced MMP1 expression [38]. However, whether miR-145 could trigger the transcriptional repression of MMP1 based on the sequence complementarity between miRNA and mRNA remains to be determined. Our results offer direct evidence of the physical interaction between miR-145 and the 3′- and 5′-UTRs of *MMP1* mRNA, demonstrating that MMP1 is a direct downstream target of miR-145. Thus, miR-145 could belong to a novel class of microRNAs that bind both the 3′- and 5′-UTRs of target transcripts [40]. According to thermodynamic analysis using

the BiBiServ-RNA hybrid database, miR-145 seemed to bind more strongly to the 5′-UTR of *MMP-1* than to its 3′-UTR. In addition, dual-luciferase reporter assays confirmed that miR-145 only slightly reduced the luciferase activity from the *MMP1* 3′-UTR, whereas plasmids containing both the 3′- and 5′-UTRs exhibited a significant decrease in luciferase activity, suggesting that this dual binding had a synergistic effect on the transcriptional repression of MMP1. These observations also indicate that the miR-145–MMP1 binding pattern differs fundamentally from a conventional 3′-UTR binding mode; in other words, they may explain why the prediction database ignores the possibility of *MMP1* being a target gene of miR-145.

MMP1 has been shown to participate in the early stages of metastatic progression in multiple cancer types by altering the extracellular matrix to facilitate cancer invasion [10,39]. In addition, the data show that MMP1 expression is increased in CSC subsets (CD133^{+}/ side-cell population) [17] and is positively correlated with the levels of cancer stem markers including CD44 [18] and SOX2 [41], suggesting that MMP1 could be involved in the regulation of cancer stemness, and warrant further functional study. Here, we observed that MMP1 expression was significantly upregulated in IMQ-treated cancer cells, and silencing it impeded IMQ-induced cancer cell stemness, suggesting that MMP1 could have a role as a critical mediator of cancer stemness. Regarding the mechanism through which MMP1 participates in cancer stemness regulation, our work focused exclusively on the miR-145–MMP1 axis and did not comprehensively assess downstream signaling pathways of MMP1 associated with stemness regulation. Thus, these should be explored in future studies.

Cancer cells with high stemness properties exhibit increased chemoresistance [4]. Here, we confirmed that in glioma cells and colon cancer cells, IMQ favored the acquisition of stem cell-like properties and decreased sensitivity to chemotherapeutic agents. Of note, the miR-145–MMP1 axis was also involved in IMQ-mediated chemoresistance, and MMP1 knockdown reversed the chemoresistance after IMQ treatment, consistent with previous findings in pancreatic cancer cells treated with 5-fluorouracil [42]. Furthermore, our experimental data were supported by the results of several previous studies, in which MMP1 was positively correlated with the expression of chemoresistance-related genes [43,44]. Regarding the mechanisms by which MMP1 contributes to chemoresistance, Hanrahan et al. [43] previously highlighted the relevance of EMT in driving docetaxel-resistant prostate cancer; thus, we cannot exclude the possibility that MMP1 regulates chemoresistance through EMT induction. Consequently, future studies should explore the association between metastasis-related factors (e.g., MMPs), stemness regulation, and the chemosensitivity of cancer cells.

## 5. Conclusion

In this study, we demonstrated that IMQ facilitates the acquisition of stem cell-like properties and chemoresistance via the upregulation of MMP1 and downregulation of miR-145, whereas miR-145-mediated downregulation of MMP1 restricted the effects of IMQ, suggesting that the miR-145–MMP1 axis is involved in the regulation of cancer stemness and chemoresistance. Our data also indicate that the miR-145–MMP1 axis serves as a potential connecting point among cancer stemness, chemoresistance, and metastasis and thus has the potential to be a crucial cancer therapeutic target.

### CRediT authorship contribution statement

**Shan Zhu**: Conceptualization, Methodology, Formal analysis, Visualization, Writing – original draft. **Ning Yang**: Investigation, Formal analysis, Visualization, Writing – review & editing. **Chao Niu**: Investigation, Formal analysis, Resources. **Wan Wang**: Investigation, Validation. **Xue Wang**: Investigation, Validation. **Junge Bai**: Validation. **Yuan Qiao**: Validation. **Shuanglin Deng**: Validation. **Yi Guan**: Funding
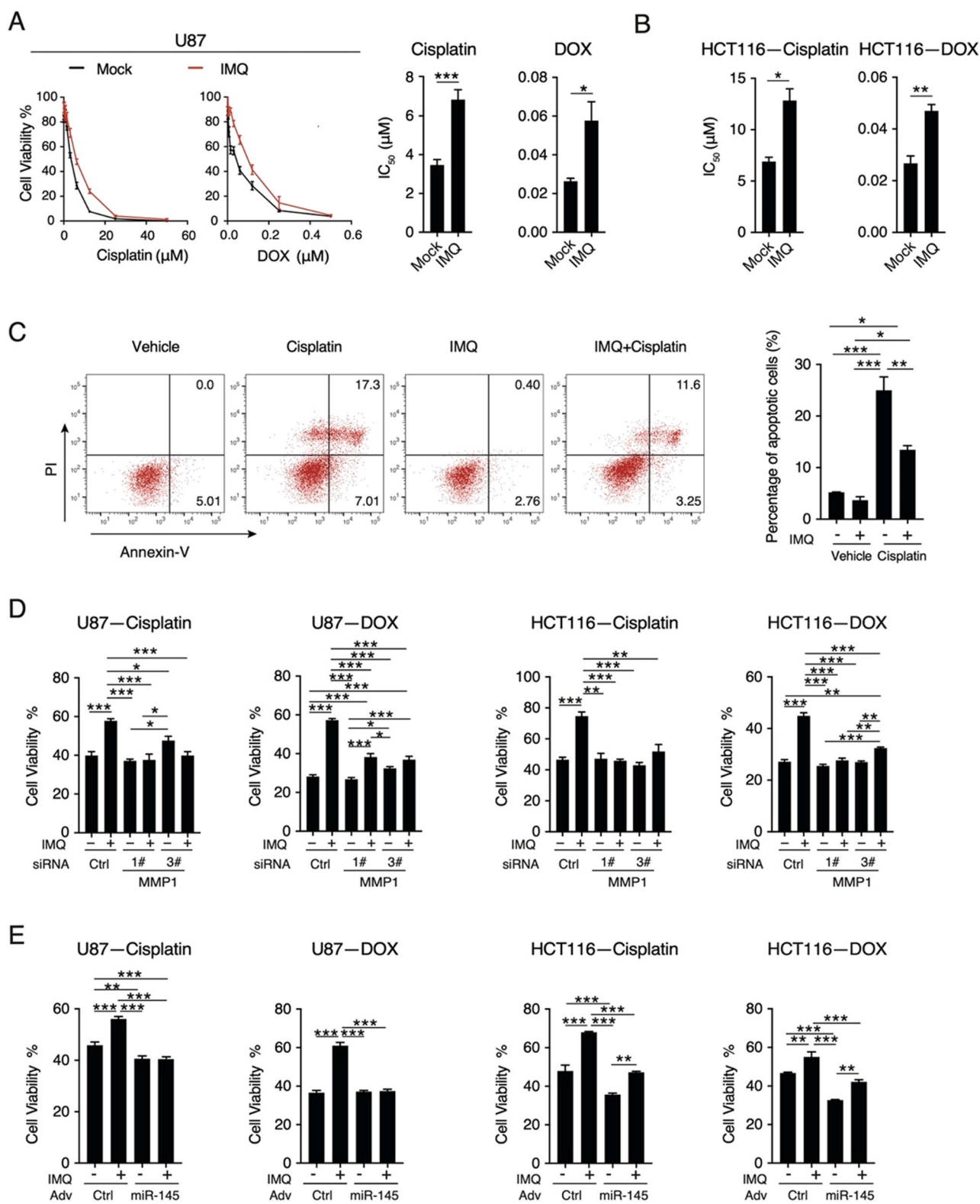
**Fig. 5.** Matrix metalloproteinase 1 (MMP1) silencing attenuates resistance to chemotherapeutic agents in imiquimod (IMQ)-treated cancer cells. (A–B) Cell viability and half-maximal inhibitory concentrations ($IC_{50}$) values in IMQ-treated U87 and HCT116 cells receiving different concentrations of cisplatin and doxorubicin (DOX). Cell viability and $IC_{50}$ values were determined via MTT assays. (C) Apoptotic response of IMQ-treated U87 cells after 3 μM cisplatin treatment for 48 h. Annexin V/PI staining for the detection of apoptotic cells. The percentage of total apoptotic cells was quantified for each sample as the sum of early and late apoptotic cells. (D–E) Cell viability of U87 and HCT116 cells treated with cisplatin (6.25 μM) and DOX (0.06 μM) after treatment with IMQ and MMP1 siRNA or control siRNA. Values in (A–E) are from three independent experiments and are presented as the mean ± SEM; * $p < 0.05$, ** $p < 0.005$, *** $p < 0.0005$. Unpaired *t*-test (A–B); one-way ANOVA with Tukey's multiple comparison test (C–E).
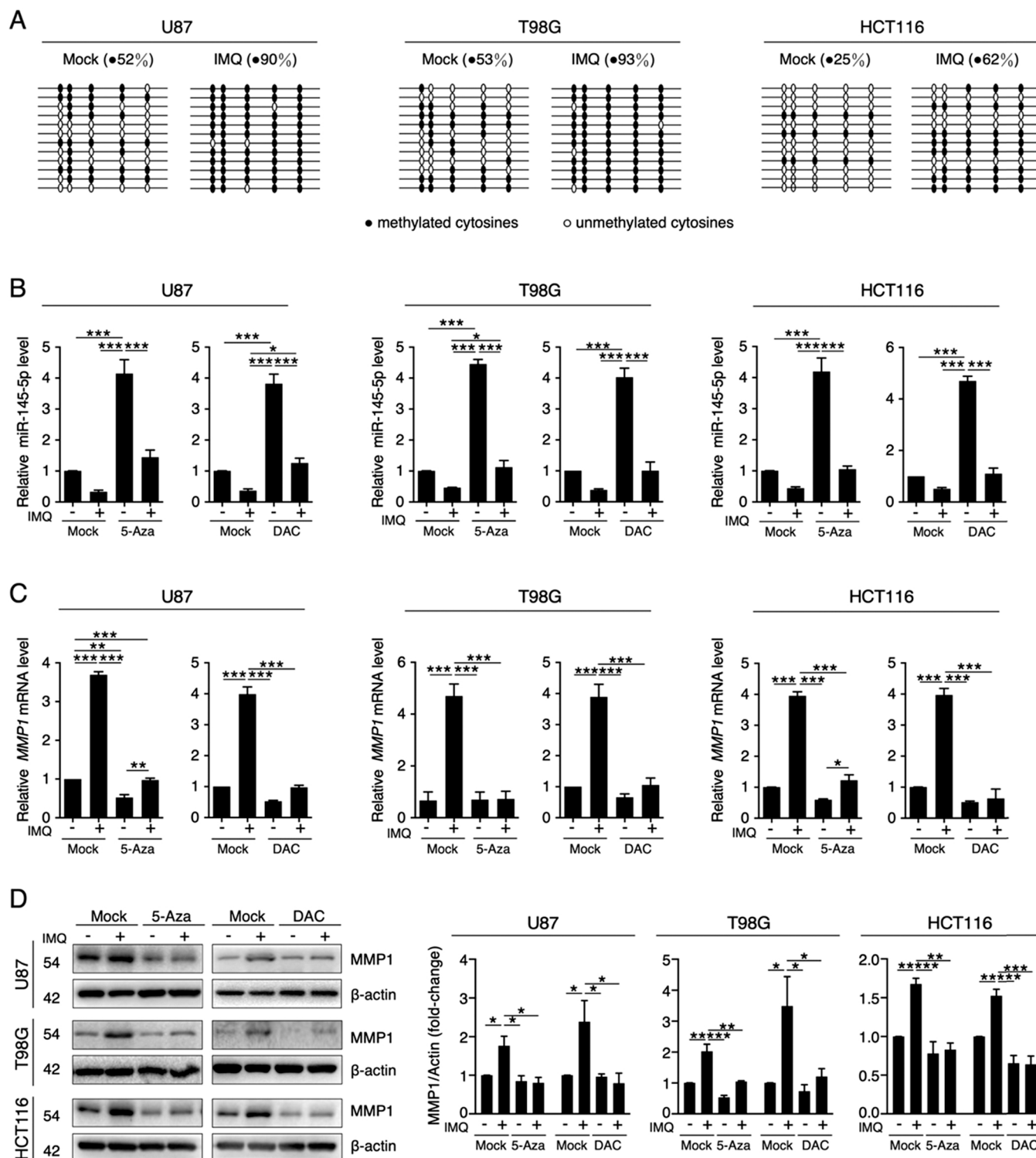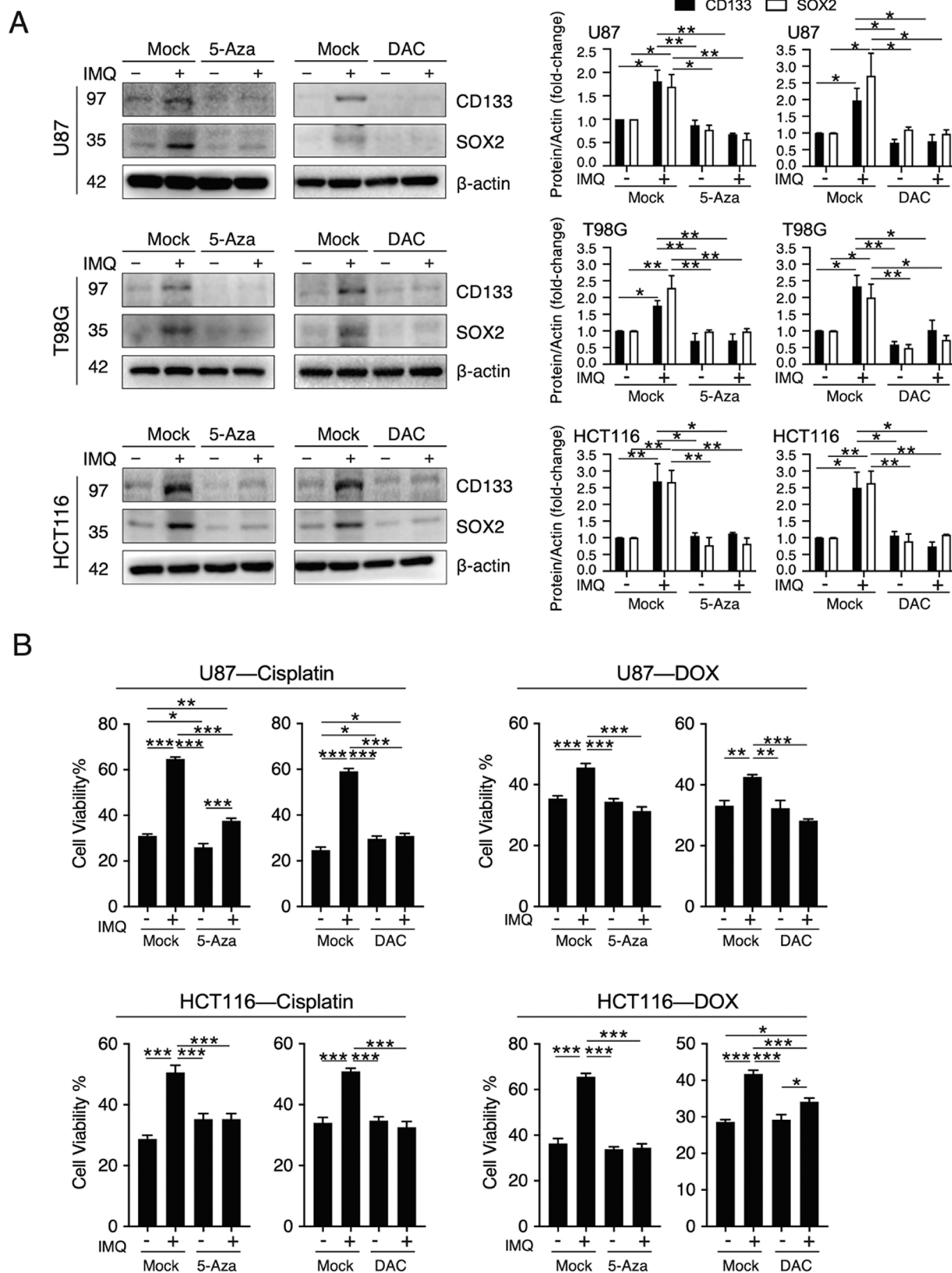
**Fig. 6.** Imiquimod (IMQ) downregulates miR-145 by facilitating DNA methylation at its promoter. (A) DNA methylation analysis of promoter fragments within the miR-145 gene in cancer cells treated with 5 μg/mL IMQ or controls. The CpG methylation ratio at each CpG site was measured using the bisulfite repetitive element PCR technique. Each circle represents a CpG site in the primary DNA sequence (open circles, non-methylated; solid circles, methylated). (B) qPCR analysis of miR-145–5p levels in cancer cells treated with IMQ and DNA methyltransferase inhibitor 5-azacytidine (5-Aza) or decitabine (DAC). Cells were pretreated with 5 μg/mL IMQ for 48 h and then stimulated with DNA methyltransferase inhibitors (5 μM 5-Aza or 5 μM DAC) and IMQ for 3 days. (C–D) qPCR and western blot analysis of MMP1 levels in cancer cells treated with DNA methyltransferase inhibitors and IMQ. Values in (B–D) are from three independent experiments and are presented as the mean ± SEM; * $p < 0.05$, ** $p < 0.005$, *** $p < 0.0005$; one-way ANOVA with Tukey's multiple comparison test.

**Fig. 7.** DNA methyltransferase inhibitors reverse imiquimod (IMQ)-induced stemness and chemoresistance of cancer cells. (A) Western blot analysis and statistical evaluation of CD133 and SOX2 protein levels in cancer cells treated with DNA methyltransferase inhibitors and IMQ. (B) Cell viability of cancer cells treated with cisplatin and doxorubicin (DOX) after treatment with DNA methyltransferase inhibitors and IMQ. Values in (A–B) are from three independent experiments and are presented as the mean ± SEM; * $p < 0.05$, ** $p < 0.005$, *** $p < 0.0005$; one-way ANOVA with Tukey's multiple comparison test.

acquisition, Writing – review & editing. **Jingtao Chen**: Supervision, Funding acquisition, Writing – review & editing.

## Declaration of Competing Interest

## Acknowledgments

## Appendix A. Supplementary material

Supplementary data associated with this article can be found in the online version at doi:10.1016/j.phrs.2022.106196.

## References

[1] H.Y. Choi, H.R. Siddique, M. Zheng, Y. Kou, D.W. Yeh, T. Machida, C.L. Chen, D. B. Uthaya Kumar, V. Punj, P. Winer, A. Pita, L. Sher, S.M. Tahara, R.B. Ray, C. Liang, L. Chen, H. Tsukamoto, K. Machida, p53 destabilizing protein skews asymmetric division and enhances NOTCH activation to direct self-renewal of TICs, Nat. Commun. 11 (2020) 3084, https://doi.org/10.1038/s41467-020-16616-8.
[2] B. Aramini, V. Masciale, G. Grisendi, F. Bertolini, M. Maur, G. Guaitoli, I. Chrystel, U. Morandi, F. Stella, M. Dominici, K.H. Haider, Dissecting tumor growth: the role of cancer stem cells in drug resistance and recurrence, Cancers 14 (2022) 976, https://doi.org/10.3390/cancers14040976.
[3] S. Marquardt, M. Solanki, A. Spitschak, J. Vera, B.M. Putzer, Emerging functional markers for cancer stem cell-based therapies: Understanding signaling networks for targeting metastasis, Semin Cancer Biol. 53 (2018) 90–109, https://doi.org/10.1016/j.semcancer.2018.06.006.
[4] J. Xiong, L. Yan, C. Zou, K. Wang, M. Chen, B. Xu, Z. Zhou, D. Zhang, Integrins regulate stemness in solid tumor: an emerging therapeutic target, J. Hematol. Oncol. 14 (2021) 177, https://doi.org/10.1186/s13045-021-01192-1.
[5] B. Zhang, Y. Li, Q. Wu, L. Xie, B. Barwick, C. Fu, X. Li, D. Wu, S. Xia, J. Chen, W. P. Qian, L. Yang, A.O. Osunkoya, L. Boise, P.M. Vertino, Y. Zhao, M. Li, H.R. Chen, J. Kowalski, O. Kucuk, W. Zhou, J.T. Dong, Acetylation of KLF5 maintains EMT and tumorigenicity to cause chemoresistant bone metastasis in prostate cancer, Nat. Commun. 12 (2021) 1714, https://doi.org/10.1038/s41467-021-21976-w.
[6] Y. Perone, A.J. Farrugia, A. Rodriguez-Meira, B. Gyorffy, C. Ion, A. Uggetti, A. Chronopoulos, P. Marrazzo, M. Faronato, S. Shousha, C. Davies, J.H. Steel, N. Patel, A. Del Rio Hernandez, C. Coombes, G. Pruneri, A. Lim, F. Calvo, L. Magnani, SREBP1 drives Keratin-80-dependent cytoskeletal changes and invasive behavior in endocrine-resistant ERalpha breast cancer, Nat. Commun. 10 (2019) 2115, https://doi.org/10.1038/s41467-019-09676-y.
[7] M.M. Wilson, R.A. Weinberg, J.A. Lees, V.J. Guen, Emerging mechanisms by which EMT programs control metastasis, Trends Cancer 6 (2020) 775–780, https://doi.org/10.1016/j.trecan.2020.03.011.
[8] F. de So.elo, A.V. Kurtova, J.M. Harnoss, N. Kljavin, J.D. Hoeck, J. Hung, J. E. Anderson, E.E. Storm, Z. Modrusan, H. Koeppen, G.J. Dijkgraaf, R. Piskol, F.J. de Sauvage, A distinct role for Lgr5+ stem cells in primary and metastatic colon cancer, Nature 543 (2017) 676–680, https://doi.org/10.1038/nature21713.
[9] T. Wang, Y. Zhang, J. Bai, Y. Xue, Q. Peng, MMP1 and MMP9 are potential prognostic biomarkers and targets for uveal melanoma, BMC Cancer 21 (2021) 1068, https://doi.org/10.1186/s12885-021-08788-3.
[10] M. Javadian, T. Gharibi, N. Shekari, M. Abdollahpour-Alitappeh, A. Mohammadi, A. Hossieni, H. Mohammadi, T. Kazemi, The role of microRNAs regulating the expression of matrix metalloproteinases (MMPs) in breast cancer development, progression, and metastasis, J. Cell. Physiol. 234 (2019) 5399–5412, https://doi.org/10.1002/jcp.27445.
[11] C. Huang, Y. Li, Y. Guo, Z. Zhang, G. Lian, Y. Chen, J. Li, Y. Su, J. Li, K. Yang, S. Chen, H. Su, K. Huang, L. Zeng, MMP1/PAR1/SP/NK1R paracrine loop modulates early perineural invasion of pancreatic cancer cells, Theranostics 8 (2018) 3074–3086, https://doi.org/10.7150/thno.24281.
[12] M. Liu, Y. Hu, M.F. Zhang, K.J. Luo, X.Y. Xie, J. Wen, J.H. Fu, H. Yang, MMP1 promotes tumor growth and metastasis in esophageal squamous cell carcinoma, Cancer Lett. 377 (2016) 97–104, https://doi.org/10.1016/j.canlet.2016.04.034.
[13] R. Harati, M.G. Mohammad, A. Tlili, R.A. El-Awady, R. Hamoudi, Loss of miR-101-3p promotes transmigration of metastatic breast cancer cells through the brain endothelium by inducing COX-2/MMP1 signaling, Pharmaceuticals 13 (2020) 144, https://doi.org/10.3390/ph13070144.
[14] Y. Chen, S. Peng, H. Cen, Y. Lin, C. Huang, Y. Chen, H. Shan, Y. Su, L. Zeng, MicroRNA hsa-miR-623 directly suppresses MMP1 and attenuates IL-8-induced metastasis in pancreatic cancer, Int. J. Oncol. 55 (2019) 142–156, https://doi.org/10.3892/ijo.2019.4803.
[15] I.A. Ho, Y. Yulyana, K.C. Sia, J.P. Newman, C.M. Guo, K.M. Hui, P.Y. Lam, Matrix metalloproteinase-1-mediated mesenchymal stem cell tumor tropism is dependent on crosstalk with stromal derived growth factor 1/C-X-C chemokine receptor 4 axis, FASEB J. 28 (2014) 4359–4368, https://doi.org/10.1096/fj.14-252551.
[16] I.A. Ho, K.Y. Chan, W.H. Ng, C.M. Guo, K.M. Hui, P. Cheang, P.Y. Lam, Matrix metalloproteinase 1 is necessary for the migration of human bone marrow-derived mesenchymal stem cells toward human glioma, Stem Cells 27 (2009) 1366–1375, https://doi.org/10.1002/stem.50.
[17] M. Nakamura, X. Zhang, Y. Mizumoto, Y. Maida, Y. Bono, M. Takakura, S. Kyo, Molecular characterization of CD133+ cancer stem-like cells in endometrial cancer, Int. J. Oncol. 44 (2014) 669–677, https://doi.org/10.3892/ijo.2013.2230.
[18] M. Sun, W. Zhou, Y.Y. Zhang, D.L. Wang, X.L. Wu, CD44+ gastric cancer cells with stemness properties are chemoradioresistant and highly invasive, Oncol. Lett. 5 (2013) 1793–1798, https://doi.org/10.3892/ol.2013.1272.
[19] M. Ashrafizadeh, A. Zarrabi, K. Hushmandi, M. Kalantari, R. Mohammadinejad, T. Javaheri, G. Sethi, Association of the epithelial-mesenchymal transition (EMT) with cisplatin resistance, Int. J. Mol. Sci. 21 (2020) 4002, https://doi.org/10.3390/ijms21114002.
[20] J. Haerinck, G. Berx, Partial EMT takes the lead in cancer metastasis, Dev. Cell 56 (2021) 3174–3176, https://doi.org/10.1016/j.devcel.2021.11.012.
[21] S.Y. Liu, X.Y. Li, W.Q. Chen, H. Hu, B. Luo, Y.X. Shi, T.W. Wu, Y. Li, Q.Z. Kong, H. D. Lu, Z.X. Lu, Demethylation of the miR145 promoter suppresses migration and invasion in breast cancer, Oncotarget 8 (2017) 61731–61741, https://doi.org/10.18632/oncotarget.18686.
[22] P. Pidikova, R. Reis, I. Herichova, miRNA clusters with down-regulated expression in human colorectal cancer and their regulation, Int. J. Mol. Sci. 21 (2020) 4633, https://doi.org/10.3390/ijms21134633.
[23] K. Skjefstad, C. Johannessen, T. Grindstad, T. Kilvaer, E.E. Paulsen, M. Pedersen, T. Donnem, S. Andersen, R. Bremnes, E. Richardsen, S. Al-Saad, L.T. Busund, A gender specific improved survival related to stromal miR-143 and miR-145 expression in non-small cell lung cancer, Sci. Rep. 8 (2018) 8549, https://doi.org/10.1038/s41598-018-26864-w.
[24] L. Shi, B. Wang, X. Gu, S. Zhang, X. Li, H. Zhu, miR-145 is a potential biomarker for predicting clinical outcome in glioblastomas, J. Cell. Biochem. 120 (2018) 8016–8020, https://doi.org/10.1002/jcb.28079.
[25] N. Arrighetti, G.L. Beretta, miRNAs as therapeutic tools and biomarkers for prostate cancer, Pharmaceutics 13 (2021) 380, https://doi.org/10.3390/pharmaceutics13030380.
[26] A.A. Balachandran, L.M. Larcher, S. Chen, R.N. Veedu, Therapeutically significant microRNAs in primary and metastatic brain malignancies, Cancers 12 (2020) 2534, https://doi.org/10.3390/cancers12092534.
[27] S. Donzelli, F. Mori, T. Bellissimo, A. Sacconi, B. Casini, T. Frixa, G. Roscilli, L. Aurisicchio, F. Facciolo, A. Pompili, M.A. Carosi, E. Pescarmona, O. Segatto, G. Pond, P. Muti, S. Telera, S. Strano, Y. Yarden, G. Blandino, Epigenetic silencing of miR-145-5p contributes to brain metastasis, Oncotarget 6 (2015) 35183–35201, https://doi.org/10.18632/oncotarget.5930.
[28] H. Shen, J. Shen, L. Wang, Z. Shi, M. Wang, B.H. Jiang, Y. Shu, Low miR-145 expression level is associated with poor pathological differentiation and poor prognosis in non-small cell lung cancer, Biomed. Pharmacother. 69 (2015) 301–305, https://doi.org/10.1016/j.biopha.2014.12.019.
[29] M. Avgeris, K. Stravodimos, E.G. Fragoulis, A. Scorilas, The loss of the tumour-suppressor miR-145 results in the shorter disease-free survival of prostate cancer patients, Br. J. Cancer 108 (2013) 2573–2581, https://doi.org/10.1038/bjc.2013.250.
[30] J.F. Zeng, X.Q. Ma, L.P. Wang, W. Wang, MicroRNA-145 exerts tumor-suppressive and chemo-resistance lowering effects by targeting CD44 in gastric cancer, World J. Gastroenterol. 23 (2017) 2337–2345, https://doi.org/10.3748/wjg.v23.i13.2337.
[31] Z. Xu, X. Zeng, J. Xu, D. Xu, J. Li, H. Jin, G. Jiang, X. Han, C. Huang, Isorhapontigenin suppresses growth of patient-derived glioblastoma spheres through regulating miR-145/SOX2/cyclin D1 axis, Neuro-Oncology 18 (2016) 830–839, https://doi.org/10.1093/neuonc/nov298.
[32] Y. Jia, H. Liu, Q. Zhuang, S. Xu, Z. Yang, J. Li, J. Lou, W. Zhang, Tumorigenicity of cancer stem-like cells derived from hepatocarcinoma is regulated by microRNA-145, Oncol. Rep. 27 (2012) 1865–1872, https://doi.org/10.3892/or.2012.1701.
[33] W. Gao, C. Zhang, W. Li, H. Li, J. Sang, Q. Zhao, Y. Bo, H. Luo, X. Zheng, Y. Lu, Y. Shi, D. Yang, R. Zhang, Z. Li, J. Cui, Y. Zhang, M. Niu, J. Li, Z. Wu, H. Guo, C. Xiang, J. Wang, J. Hou, L. Zhang, R.F. Thorne, Y. Cui, Y. Wu, S. Wen, B. Wang, Promoter methylation-regulated miR-145-5p inhibits laryngeal squamous cell carcinoma progression by targeting FSCN1, Mol. Ther. 27 (2019) 365–379, https://doi.org/10.1016/j.ymthe.2018.09.018.
[34] C. Patinote, N.B. Karroum, G. Moarbess, N. Cirnat, I. Kassab, P.A. Bonnet, C. Deleuze-Masquefa, Agonist and antagonist ligands of toll-like receptors 7 and 8: ingenious tools for therapeutic purposes, Eur. J. Med. Chem. 193 (2020), 112238, https://doi.org/10.1016/j.ejmech.2020.112238.
[35] H. Chi, C. Li, F.S. Zhao, L. Zhang, T.B. Ng, G. Jin, O. Sha, Anti-tumor activity of toll-like receptor 7 agonists, Front. Pharmacol. 8 (2017) 304, https://doi.org/10.3389/fphar.2017.00304.
[36] S. Zhu, N. Yang, Y. Guan, X. Wang, G. Zang, X. Lv, S. Deng, W. Wang, T. Li, J. Chen, GDF15 promotes glioma stem cell-like phenotype via regulation of ERK1/2-c-Fos-LIF signaling, Cell Death Discov. 7 (2021) 3, https://doi.org/10.1038/s41420-020-00395-8.

[37] B. Ding, M. Yao, W. Fan, W. Lou, Whole-transcriptome analysis reveals a potential hsa_circ_0001955/hsa_circ_0000977-mediated miRNA-mRNA regulatory sub-network in colorectal cancer, Aging 12 (2020) 5259–5279, https://doi.org/10.18632/aging.102945.

[38] A.S. Azmi, Y. Li, I. Muqbil, A. Aboukameel, W. Senapedis, E. Baloglu, Y. Landesman, S. Shacham, M.G. Kauffman, P.A. Philip, R.M. Mohammad, Exportin 1 (XPO1) inhibition leads to restoration of tumor suppressor miR-145 and consequent suppression of pancreatic cancer cell proliferation and migration, Oncotarget 8 (2017) 82144–82155, https://doi.org/10.18632/oncotarget.19285.

[39] G.A. Conlon, G.I. Murray, Recent advances in understanding the roles of matrix metalloproteinases in tumour invasion and metastasis, J. Pathol. 247 (2019) 629–640, https://doi.org/10.1002/path.5225.

[40] I. Lee, S.S. Ajay, J.I. Yook, H.S. Kim, S.H. Hong, N.H. Kim, S.M. Dhanasekaran, A. M. Chinnaiyan, B.D. Athey, New class of microRNA targets containing simultaneous 5'-UTR and 3'-UTR interaction sites, Genome Res. 19 (2009) 1175–1183, https://doi.org/10.1101/gr.089367.108.

[41] F. Oppel, N. Muller, G. Schackert, S. Hendruschk, D. Martin, K.D. Geiger, A. Temme, SOX2-RNAi attenuates S-phase entry and induces RhoA-dependent switch to protease-independent amoeboid migration in human glioma cells, Mol. Cancer 10 (2011) 137, https://doi.org/10.1186/1476-4598-10-137.

[42] L. Song, H. Liu, Q. Liu, Matrix metalloproteinase 1 promotes tumorigenesis and inhibits the sensitivity to 5-fluorouracil of nasopharyngeal carcinoma, Biomed. Pharmacother. 118 (2019), 109120, https://doi.org/10.1016/j.biopha.2019.109120.

[43] K. Hanrahan, A. O'Neill, M. Prencipe, J. Bugler, L. Murphy, A. Fabre, M. Puhr, Z. Culig, K. Murphy, R.W. Watson, The role of epithelial-mesenchymal transition drivers ZEB1 and ZEB2 in mediating docetaxel-resistant prostate cancer, Mol. Oncol. 11 (2017) 251–265, https://doi.org/10.1002/1878-0261.12030.

[44] A. Khanna, K. Mahalingam, D. Chakrabarti, G. Periyasamy, Ets-1 expression and gemcitabine chemoresistance in pancreatic cancer cells, Cell. Mol. Biol. Lett. 16 (2011) 101–113, https://doi.org/10.2478/s11658-010-0043-z.